

Single-stage ZETA-SEPIC converter for plugin Electric vehicles

Yendeti Rama krishna¹Jagarlamudi Anusha²

¹PG Scholar, Dept. of EEE, Chirala Engineering College, Chirala, India.

²Assistant Professor, Dept. of EEE, Chirala Engineering College, Chirala, India

Received 15 August 2019; Accepted 30 August 2019

Abstract: A single-stage-based integrated power electronic converter has been proposed for plug-in electric vehicles (PEVs). The proposed converter achieves all modes of vehicle operation, i.e. plug-in charging, propulsion and regenerative braking modes with wide voltage conversion ratio (M) [$M < 1$ as well as $M > 1$] in each mode. Therefore, a wide variation of battery voltage can be charged from the universal input voltage (90–260 V) and allowing more flexible control for capturing regenerative braking energy and dc-link voltage. The proposed converter has least components compared to those existing converters which have stepping up and stepping down capability in all modes. Moreover, a single switch operates in pulse width modulation in each mode of converter operation hence control system design becomes simpler and easy to implement. To correctly select the power stage switches, a loss analysis of the proposed converter has been investigated in ac/dc and dc/dc stages.

Index terms: ZETA SEPIC, Dc -Dc Converter, Electric vehicle, State of Charge (Soc)

I. INTRODUCTION

The electric vehicles or plug-in electric vehicles (PEVs) are now a promising solution to curb the air pollution that uses pollution-free battery power to produce clean energy for the vehicle [1]. The PEVs are combination of on-board charger, battery, and the inverter-drive system [2–5]. In majority of PEVs, a bidirectional dc/dc converter is interfaced between the battery and dc-link of machine inverter [6–8] for power flow during propulsion and regenerative braking operation. Therefore, an individual ac/dc converter is used to charge the battery from the grid side. In this conventional structure, two separate power electronic converters are needed for two independent operations (charging and discharging of the battery). The bidirectional dc/dc converter in conventional structure can be integrated with the on-board charger, to have one power electronics interface for complete operation of PEVs. The overall block diagram of an integrated charger with single power electronic is shown in Fig. 1a. This integration reduces the number of components because some of the switches and inductors are utilised both in ac/dc and dc/dc stages. Therefore, reduced number of switches and inductors lead to higher power density, compact size and lower cost. In this regard, this paper

proposes, a new ZETA-SEPIC-based integrated converter for PEVs, as shown in Fig. 1b which has buck/boost capability in each mode of operation. In addition, buck/boost operation in each mode allows selection of wide range of the battery voltage, efficient control of dc-link voltage and capturing the regenerative braking with a wide variation of the motor speed.

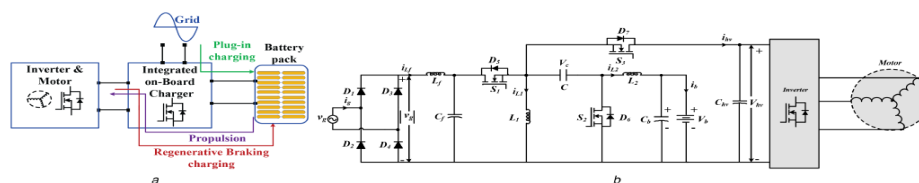


Fig. 1 Block diagram and proposed structure of the integrated converter

(a) Block diagram of PEV with on-board integrated battery charger, (b) Proposed ZETA-SEPIC-based integrated converter for PEVs.

II. OPERATION OF THE PROPOSED CONVERTER

The proposed integrated converter operates in three modes: battery charging from the grid (plug-in charging), propulsion, and regenerative braking of charging. In the following section, operation of converter is discussed in detailed manner.

a) Plug-in charging mode: The plug-in charging mode of vehicle is possible only when vehicle is not in motion and then charger plug is connected to single phase supply socket to charge the battery. In this mode, the

proposed converter operates as ZETA PFC converter and switch S_1 is pulse width modulation (PWM) gated while switch S_2 and S_3 are in OFF-state. When switch S_1 is turned ON, inductor L_1 stores energy through the path $|v_g|-L_f-S_1-L_1-|v_g|$ and inductor L_2 stores energy through the path $|v_g|-L_f-S_1-C-L_2-V_b-|v_g|$, as shown in Fig. 2a. When switch S_1 is turned OFF, inductor L_1 discharges by supplying its stored energy to the capacitor C , and voltage across capacitor gradually increases, which is shown in Fig. 2d, and this capacitor is charged to the battery voltage V_b . While inductor L_2 supplies energy to the output stage (capacitor and battery) shown in Fig. 2b and current through L_2 decreases linearly, as shown in Fig. 2d. The capacitor Chv is charged to $V_{g,max}$ through the body diode of S_3 in very short duration then after it retains this value forever in this mode. If the duty ratio of the converter is d_1 then voltage-second balance either of inductor L_1 or L_2 for one switching period, T_s , can be given as

$$V_{g,max} |\sin(\omega t)| * d_1(t) = V_b * (1 - d_1(t)) * T_s$$

$$M_1 = \frac{V_b}{V_{g,max} |\sin \omega t|} = \frac{d_1(t)}{1 - d_1(t)}$$

b) Propulsion mode: When this mode begins, battery started supplying power to the dclink of the inverter and vehicle comes in running mode. During motion of the vehicle, the SOC of the battery continuously decreases. In this mode, switches S_1 and S_3 are kept in OFF state using mode selector logic, and switch S_2 is gated through PWM signal. When switch S_2 is turned ON, inductor L_2 stores energy through the path $V_b-L_2-S_2-V_b$, and capacitor C discharges through inductor L_1 , as shown in Fig. 2a and inductor current through L_1 is

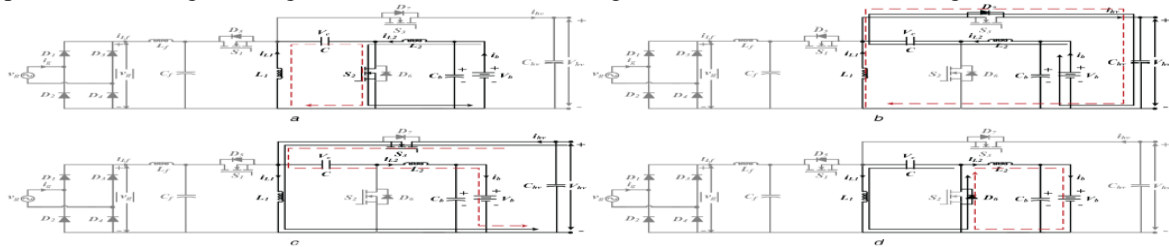


Fig. 2 Equivalent operating circuits during propulsion and regenerative braking modes

(a) Propulsion mode of operation, when switch S_2 is ON, **(b)** When switch S_2 is OFF, **(c)** Operation of regenerative braking, when switch S_3 is ON, **(d)** When switch S_3 is OFF.

linearly increases. When S_2 is turned OFF, inductor L_2 transfers its stored energy in the capacitor C and dc-link capacitor Chv through the path $V_b-L_2-C-D7-V_{hv}-V_b$ and capacitor C is charged to the battery voltage. The inductor L_1 transfers its stored energy to the dc-link through the path $L_1-D7-V_{hv}-L_1$, as shown in Fig. 2b, and current through L_1 gradually decreases,. If the duty ratio of the converter is d_2 and applying voltage-second balance either in inductor L_1 or L_2 for one switching period then one can obtain:

$$V_b * d_2 * T_s = V_{hv} * (1 - d_2) * T_s$$

$$M_2 = \frac{V_{hv}}{V_b} = \frac{d_2}{1 - d_2}$$

c) Regenerative braking mode:

Operation of regenerative braking mode is similar to the grid mode operation, when switch S_3 is turned ON, inductor L_1 stores energy through the path $V_{hv} S_3-L_1-V_{hv}$ and inductor L_2 stores energy through the path $V_{hv}-S_3-C-L_2-V_b-V_{hv}$, as shown Fig. 2c. When S_3 is turned OFF L_1 transfers its stored energy to the capacitor (C) through the path $C-L_1-D_6$ as shown in Fig. 2d and capacitor voltage V_c gradually increases, While, L_2 transfers its stored energy to capacitor C_b and battery (Fig. 2d). If the duty ratio of the converter is d_3 by applying voltage-second balance either of inductor L_1 or L_2 , and one can obtain:

$$V_{hv} * d_3 * T_s = V_b * (1 - d_3) * T_s$$

$$M_3 = \frac{V_b}{V_{hv}} = \frac{d_3}{1 - d_3}$$

III. CONTROL SYSTEM DESIGN

The control structure during different modes of converter operation [10] is shown in Fig. 3. Each mode is implemented by mode selector logic, which requires external input such as torque τ ,

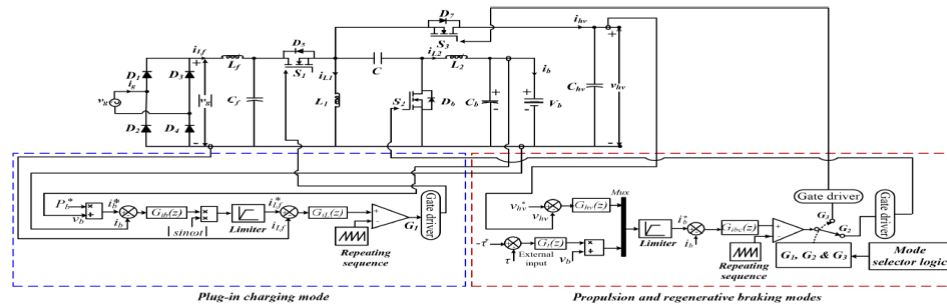


Fig. 3 Control algorithm of the proposed converter during different modes

speed ω , and charging power P_g . Since this work is focused on power electronics converter parts of the electric vehicle; therefore, the mode selection is done manually. During battery charging from the grid, the reference charging power is divided by instantaneous battery voltage, which is input to the outer proportional-integral (PI) controller $G_{ib}(z)$. The output of the outer PI controller is a reference dc signal for inner controller $G_{il}(z)$, and multiplied by a unit rectified sinusoidal wave to generate the final reference input to inner current PI controller. The inner current controller is used for the correction of power factor at the grid side. The output controller $G_{ib}(z)$ is expressed as

$$G_{ib}(z) = K_p + \frac{K_i T_s}{z - 1}$$

where K_p is the proportional gain to adjust the control bandwidth and K_i is the integral gain to achieve zero steady-state error. The inner PI controller is given by the following equation as

$$G_{il}(z) = K_{pc} + \frac{K_{ic} T_s}{z - 1}$$

where K_{pc} is the proportional gain and K_{ic} is the integral gain. These two coefficients should be tuned such that the bandwidth of the controller is kept between one-sixth to one-tenth of the switching frequency. Further, due to presence of low frequency components (100 Hz) in battery current, the bandwidth of $G_{ib}(z)$ controller is kept <100 Hz to avoid the distortion in the reference signal for inner current loop. In propulsion and regenerative braking mode of operation, average current mode controller is used. Depending upon operating modes appropriate switches are turned ON. In propulsion mode, the dc-link voltage is regulated through two-loop controller. The outer PI controller $G_{hv}(z)$ regulates the dc-link voltage by generating reference battery current for the inner current controller $G_{bc}(z)$, which is provided by the average current mode controller. In regenerative braking modes, the reference quantity is usually torque. Therefore, torque is converted into reference charging power and this reference power is divided by instantaneous battery voltage, to generate reference battery current, which is input to the current controller $G_{bc}(z)$ for battery current tracking and as shown in Fig. 3.

IV. SIMULATION RESULTS

The simulation of the proposed converter has been verified in MATLAB/SIMULINK environment with two sets of circuit parameters, as shown in Table .

grid voltage (V_g)	220/70.7 V
DC-link voltage (V_{hv})	400/100 V
line frequency (f_L)	50/50 Hz
battery nominal voltage (V_b)	300/60 V
nominal charging power (P_b)	1 kW/230 W
L_1/L_2	2/2 mH
switching frequency (f_s)	20/20 kHz
$C_h/C_i/C_b$	SET1 = SET2 = 550/10/2200 μ F

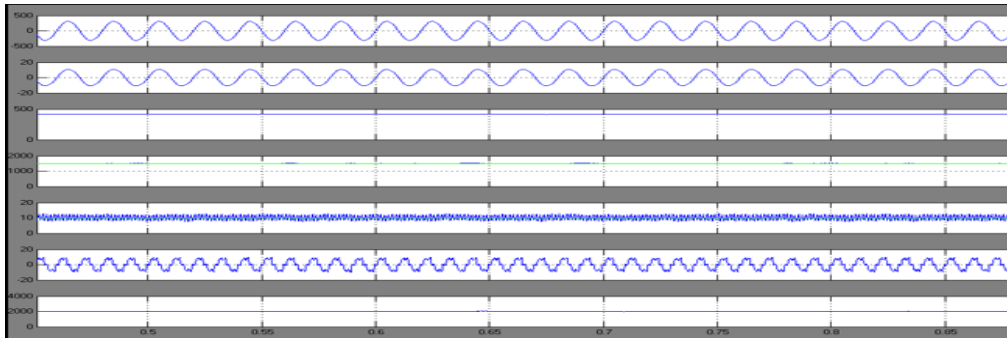


Fig. 4 Simulation results

Simulation waveforms during plug-in charging mode with 220 VRMS of grid voltage, Waveforms of v_g , i_g , V_c , I_L , V_c and motor current and speed.

V. CONCLUSION

The proposed converter has buck/boost operation in each mode of converter operation without voltage reversal which allows selection of a wide range of the battery voltage, efficient control of dc-link voltage and capturing the regenerative braking energy with wide variations of the motor speed. In comparison with existing single-stage converters, the proposed converter has the least component to those converters which have buck/boost operation in each mode.

REFERENCES

- [1]. Chan, C.C., Chau, K.T.: 'An overview of power electronics in electric vehicles', *IEEE Trans. Ind. Electron.*, 1997, **44**, (1), pp. 3–13
- [2]. Emadi, A., Lee, Y.J., Rajashekara, K.: 'Power electronics and motor drives in electric, hybrid electric, and plug-in hybrid electric vehicles', *IEEE Trans. Ind. Electron.*, 2008, **55**, (6), pp. 2237–2245
- [3]. Singh, A.K., Pathak, M.K.: 'An improved two-stage non-isolated converter for on-board plug-in hybrid EV battery charger'. IEEE 1st Int. Conf. Power Electronics, Intelligent Control and Energy Systems (ICPEICES), 2016. pp. 1–6
- [4]. Musavi, F., Edington, M., Eberle, W., *et al.*: 'Evaluation and efficiency comparison of front end ac-dc plug-in hybrid charger topologies', *IEEE Trans. Smart Grid*, 2012, **3**, (1), pp. 413–421
- [5]. McGrath, B.P., Holmes, D.G., McGoldrick, P.J., *et al.*: 'Design of a softswitched 6-kW battery charger for traction applications', *IEEE Trans. Power Electron.*, 2007, **22**, (4), pp. 1136–1144

Yendeti Rama krishna. "Single-stage ZETA-SEPIC converter for plugin Electric vehicles." IOSR Journal of Engineering (IOSRJEN), vol. 09, no. 08, 2019, pp. 09-12.